Chapter 4

Carbon Dioxide Utilization and Sequestration in Kerogen Nanopores

Cudjoe Sherifa and Barati Reza

Additional information is available at the end of the chapter

http://dx.doi.org/10.5772/intechopen.78235

Abstract

Carbon dioxide (CO_2) has been injected into oil reservoirs to maximize production for decades. On the other hand, emitted CO_2 from industrial processes is captured and stored in geological formations to mitigate greenhouse gas effects. As such, greater attention is drawn to the potential of utilizing the captured CO_2 in EOR processes. A significant portion of the injected CO_2 remains trapped due to capillary forces and through dissolution in residual liquids. In organic-rich shales, the presence of isolated kerogen nanopores add to the sequestration process due to the adsorptive nature of the surface and its preference to CO_2 over methane (CH_4), in addition to the sealing capacities of these formations. This work summarizes the latest findings of the literature with the purpose of defining further areas of investigation to fully capitalize on the potential of CO_2 sequestration and utilization in kerogen nanopores.

Keywords: CCUS, enhanced oil recovery, organic-rich shales, anthropogenic CO_2, kerogen nanopores

1. Introduction

Carbon dioxide capture, utilization and storage (CCUS) technologies involve capturing carbon dioxide (CO_2) emissions to create a synergy between the high demand for fossil fuel and mitigating greenhouse gas effects at the lowest possible cost.

CCUS captures over 90% of CO_2 emissions from power plants and industrial facilities and is predicted to reduce global gas emissions by 14% in 2050. Bearing in mind that, fossil fuel-fired power plants in the United States account for 30% of U.S. total greenhouse gas (GHG) emissions, which will only continue to increase regardless [1]. The capacity of CO_2 utilization

and storage in the U.S. is approximately 30 billion metric tons, equivalent to 35 years of CO_2 emissions captured from 140 Gigawatts (GWs) of coal-fired power [2, 3].

The captured CO_2 emissions are usually injected into geologic formations such as deep saline aquifers for storage, but most recently associated with enhanced oil recovery (CO_2-EOR) in oil and gas reservoirs. Although, CO_2-EOR has been practiced for decades now, recent advances combine the recovery process with CO_2 sequestration.

CO_2-EOR involves the injection of CO_2 into an oil/gas reservoir to recover more hydrocarbons (oil and/ or gas). Mostly, the volume of the injected CO_2 differs from that of the produced fluid with CO_2, indicating trapping or storage. Hence, incorporating the storage of anthropogenic CO_2 into CO_2-EOR in already developed oil and gas reservoirs seems economically and technically feasible. Different forms of trapping mechanisms, such as hydrodynamic and capillary trapping hold the CO_2 in place to prevent movement/leakage, ubiquitous to almost all oil and gas reservoirs [2, 3].

The United States (US) leads the world in both the number of CO_2-EOR projects and in the volume of CO_2-EOR oil production due to complimentary geology (low thermal gradient and high permeability) in the Permian Basin, located in West Texas and southeastern New Mexico [4]. Approximately 11 trillion cubic feet (560 million metric tons) total volume of CO_2 is utilized in by US CO_2-EOR as compared to 100 trillion cubic feet (5090 million metric tons) per year of total US CO_2 emissions from industrial sources [1, 4–6].

Although, CO_2 storage during CO_2-EOR in conventional oil and gas reservoirs is proven effective, the potential to sequester in unconventional organic-rich shales (gas/oil) is even more promising and economical, yet there has been minimum attention given to these vast resources. Organic-rich shales are naturally suited for CO_2 storage due to the ultra-tight impermeable nature of the formation, which would curtail CO_2 leakage. Moreover, the adsorptive surface of kerogen and kerogen nanopores in shales can store substantial amounts of CO_2 in its adsorbed state [5–7]. Thus, in depleted shale gas reservoirs, injected CO_2 replaces methane (CH_4) in the kerogen micro and nanopores and adsorb to the kerogen surface for storage [7–9]. This chapter therefore investigates the potential of CO_2 sequestration in kerogen nanopores.

2. Carbon capture

Carbon capture technology started in the 1970s in North America at industrial projects before it was applied to power generation [1]. Early application of carbon capture on a commercial basis was focused on the removal of CO_2 as part of certain industrial processes in concentrated streams [1, 8]. The Department of Energy (DOE) estimates that approximately 30 million metric tons per year of pure CO_2 are currently produced at industrial facilities located within 50 miles of existing CO_2 pipeline networks [10].

Some industrial processes with large-scale carbon capture in commercial operation include coal gasification, ethanol production, fertilizer production, natural gas processing, refinery hydrogen production, and coal-fired power generation [7, 10].

- Natural sources of CO_2 are made up of underground accumulations of naturally occurring gases with 90% CO_2. As of 2015, the natural sources are projected to account for approximately 65 Mt/a of CO_2 [8].
- Natural-gas processing are also naturally occurring underground accumulations but with significant methane content. The contribution of natural-gas processing has increased from 5 Mt/a of CO_2 in 2000 to a projected 20 Mt/a of CO_2 in 2015 [8]. Some of the known challenges of natural-gas processing include: higher oxygen (O_2) content, lower CO_2 concentration, higher flue gas and high flame temperatures [1].
- Hydrocarbon conversion involves the conversion of crude oil (or hydrocarbon feedstock) into several (high-value) products to capture CO_2 as a by-product. This process is projected to increase to approximately 5 Mt/a based on known projects under construction and in final phase [8].

However, with the recent inclusion of power generation, new systems are designed to capture and concentrate CO_2 using the following processes [7]:

- Pre-combustion carbon capture

Fuel undergoes gasification instead of combustion to produce syngas made of carbon monoxide (CO) and hydrogen (H_2). Carbon monoxide (CO) is then converted to CO_2 through a later shift reaction, while a solvent separates the CO_2 from H_2. The pre-combustion carbon capture is mostly combined with an integrated gasification combined cycle (IGCC) power plant to burn the H_2 in a combustion turbine and the resulting exhaust heat, used to power a steam turbine [1, 6].

- Post-combustion carbon capture

It involves the use of chemical solvents to separate CO_2 from the resulting flue gas from fossil fuel combustion. This method is commonly used by modified power plants for carbon capture [7].

- Oxyfuel carbon capture

This process requires the combustion of fossil fuel in pure oxygen to render the CO_2-rich exhaust gas for capture [7].

In 2016, the US Energy Information Administration (EIA) reported that electricity generated from natural gas is expected to exceed that of coal for the first time [9]. This calls for more effective measures to be put in place to curtail greenhouse gas (GHG) effects.

2.1. Carbon capture benchmarks

There are about 21 commercial-scale carbon capture projects around the world with 22 more in development [7]. Below is a list of a few of the many benchmarks in carbon capture:

- As of 2017, the Archer Daniels Midland (ADM) Company captures CO_2 from Biofuels (ethanol) production, and stores in the Mt. Simon Sandstone, a deep saline formation, Decatur, IL. An estimated amount of 1.1 million tons of CO_2 is captured per year [1, 3].

- In 2017, the NRG Petra Nova Project, TX, captures 90% of CO_2 (approximately, 1.6 million tons of CO_2 per year) from a 240 MW slipstream of flue gas of existing WA Parish plant, and transported to a nearby oil field [7].
- In 2016, Abu Dhabi CCS Project Phase 1: Emirates Steel Industries, an operating iron and steel plant, used to capture CO_2 for enhanced oil recovery by the Abu Dhabi National Oil Company (ADNOC) [3, 5].
- In 2015, Shell Quest Project, AB, CA, a bitumen upgrader complex, captures about 1 million tons of CO_2 annually from hydrogen production units and injects it into a deep saline formation for sequestration [7].
- In 2013, Conestoga Energy Partners/Petro-Santander Bonanza Bioethanol plant, KS, an ethanol plant, captures and supplies approximately 100,000 tons of CO_2 per year to a Kansas EOR field [1, 5].
- In 2010, Occidental Petroleum's Century Plant (OPCP), TX, a natural gas processing facility, compresses and transports CO_2 stream for utilization in the Permian Basin, among others [3, 5].

3. Carbon dioxide utilization (CO_2: EOR)

CO_2-EOR has been successfully implemented for nearly half a century now to recover additional oil from developed conventional oil fields in the United States and around the world. It involves the injection of CO_2, either in its supercritical or gaseous state to re-pressurize a depleted reservoir pressure to cause residual oil held in the smaller pores by capillary forces to be released [9, 10]. CO_2, unlike other fluids, reaches miscibility with crude oil at lower pressures. Furthermore, it is less expensive than other miscible fluids. As such the injected CO_2 becomes soluble with the residual oil as light hydrocarbons from the oil dissolve in the CO_2 while the CO_2 density is high when oil contains a significant volume of light hydrocarbons [4, 11].

Upon discovery, an oil reservoir is initially produced by means of the pressure gradients within the reservoir that provides the energy to move reservoir fluids to the surface. This is called the primary production stage. Eventually, the reservoir pressure declines and flow to the wellbore ceases. At this moment, a range of secondary or tertiary (EOR) methods are implemented to recover additional volumes of oil. The primary stage only recovers about 5–20% of the original oil-in-place (OOIP), with considerable amount of oil left trapped in the pore spaces of the rock [9, 12].

The next stage of production is the secondary recovery, which involves the injection of a fluid, either gas or water to sustain and maintain the depleted reservoir drive, and simultaneously recover substantial amounts of the remaining OOIP. Treated produced water (waterflooding) is commonly used at this stage since it is less expensive and readily available. In most cases, the water bypasses the oil due to difference in viscosity leaving behind significant amounts of the remaining oil-in-place. Waterflooding results in approximately 50–60% of the OOIP

trapped, hence the need for CO_2-EOR in most oil reservoirs already replenished with water-flooding. Both primary and secondary recovery methods usually extract about 35% of the OOIP [4, 9, 10].

To produce more of the remaining oil-in-place, a tertiary oil recovery phase is implemented, where fluids (CO_2, nitrogen, enriched gas, polymer solutions or surfactant solutions) are injected to interact with the oil and cause substantial changes to the oil properties [12]. Carbon dioxide (CO_2) flooding is one of the most proven EOR methods, where CO_2 is injected either in its gaseous or supercritical state. The injected CO_2 is determined to reduce the interfacial tension, minimize the viscosity of the oil to make it lighter, cause the oil volume to swell, and eventually cause the oil to flow more freely within the reservoir to the producer wellbore [11].

CO_2 is mostly delivered to the field at a high pressure (>1200 psi) and density (5 lb. /gal) into injection wells within a designed pattern based on computer simulation to optimize areal sweep of the reservoir [13, 14]. Miscibility of CO_2 with the oil is important as it causes the physical forces (interfacial tension) holding the two phases apart to disappear. It occurs at a minimum pressure (MMP), where about 95% of the OOIP is recovered. Below the minimum miscibility pressure (MMP), CO_2 and oil will no longer be miscible, the oil and gas phases separate, thereby decreasing oil production rate. Significant volumes of oil are produced during CO_2-EOR. For example, the Wasson field, a Denver unit CO_2-EOR has produced more than 120 million incremental barrels of oil through 2008, with more than 2 billion barrels of OOIP and 40% of oil remaining after Waterflooding [14, 15, 19]. All types of oil reservoirs, either carbonates or sandstone could be suitable for CO_2-EOR provided the MMP can be reached [13, 14].

The operation of a CO_2-EOR project is a closed-loop system as shown in **Figure 1**, where about half of the injected CO_2 is trapped or dissolved in the reservoir and its fluids (oil and water). The produced CO_2 with oil is separated and re-injected back into the reservoir, ensuring an increase in trapped CO_2 instead of being released to the atmosphere. In addition, CO_2-EOR provides a market and revenues for the captured CO_2 from anthropogenic (industrial and power plants) sources [14, 15]. As the project matures, the volume of injected CO_2 diminishes, while recycled volumes increase. This indicates that CO_2 is being stored in the formation through a capillary trapping mechanism [10, 13, 14].

CO_2-EOR was first tested on a large-scale in the 1970s in the Permian Basin of West Texas and southeastern New Mexico. These initial projects used separated CO_2 from processed natural gas and natural sources of CO_2 instead of anthropogenic CO_2 from industrial power plants. **Figure 2** shows CO_2-EOR projects carried out around the world and in the U.S. from the 1970s to present day [9, 16]. Three developed source fields include, Sheep Mountain in south central Colorado, Bravo Dome in northeastern New Mexico, and McElmo Dome in southwestern Colorado [10]. The recent depletion of the natural source fields of CO_2 and size limitation of the pipelines for CO_2-EOR processes have paved the way for anthropogenic supplies of CO_2. In so doing, subsequent projects employ CO_2 molecules from captured emissions to supply large quantities of CO_2 for EOR processes in oil fields. Technological advancement in CO_2-EOR applications, such as 3D seismic and geomodeling reduce the rise of failures and improves the flooding efficiency [10, 13–15].

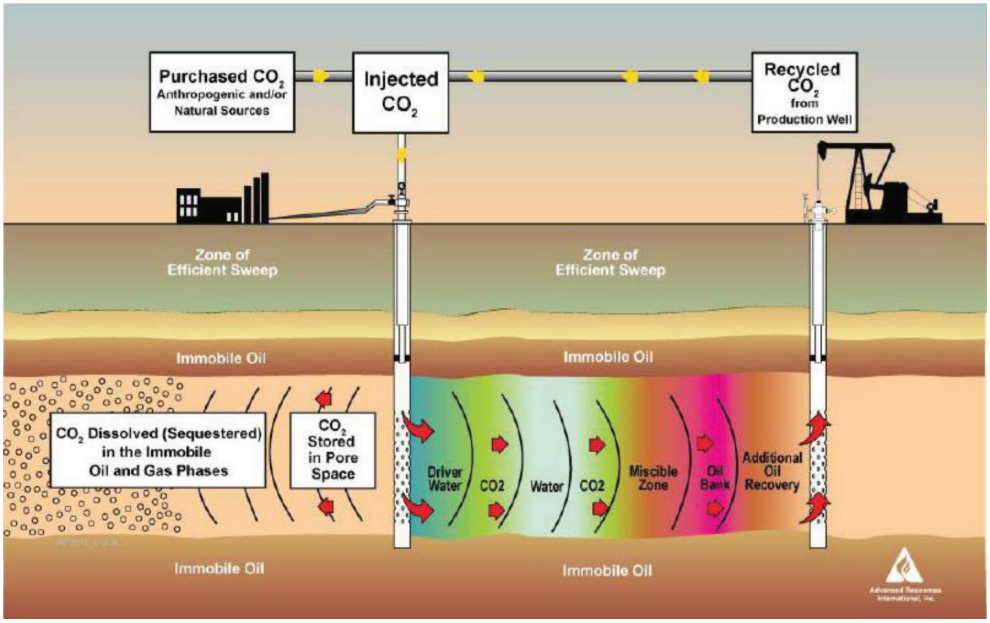

Figure 1. Schematic diagram of a closed loop CO_2-EOR [4].

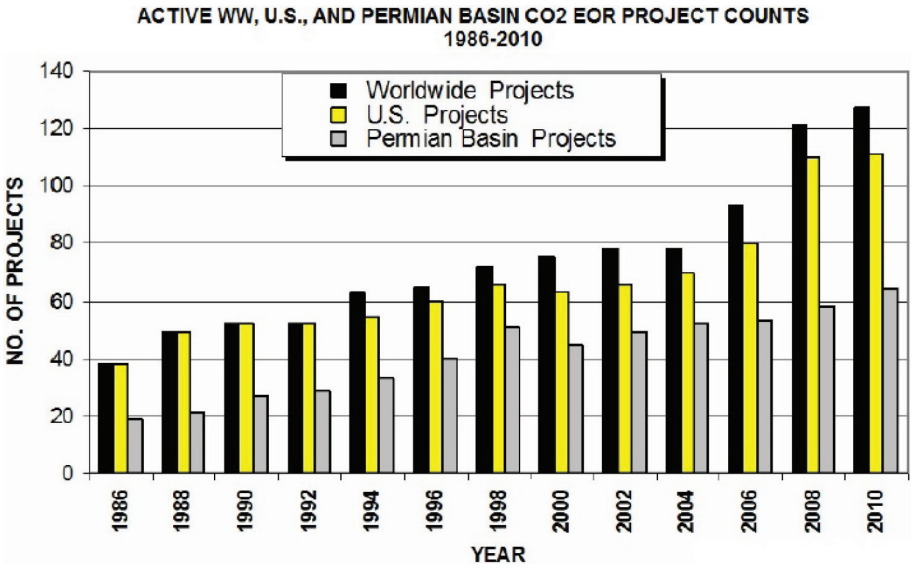

Figure 2. CO_2-EOR projects conducted worldwide and in the U.S [10].

4. Carbon dioxide sequestration

The potential of CO_2 sequestration in geologic formations is possible from the fact that certain reservoirs naturally trap and store oil and natural gas over long geological time periods until extracted [1, 4, 6, 16]. In so doing, CO_2 from power plants and industrial facilities can be trapped and stored in potential geologic formations. A large percentage of the originally injected CO_2 gets trapped in the pores of the geologic formation, while a portion of it is dissolved in the oil and also end up trapped [3, 6, 17]. These trapping processes continue as long as the CO_2 is injected. Percentage of stored CO_2 is based on total injected volumes and not on the purchased volume and is given as [10].

$$CO_{2storage}(\%) = \left(CO_{2injected} - CO_{2produced} - CO_{2losses}\right)/CO_{2purchased} \quad (1)$$

where, $CO_{2storage}$ is the CO_2 storage in metric, $CO_{2injected}$ is the total CO_2 injected, $CO_{2produced}$ is the CO_2 produced, and $CO_{2purchased}$ is the purchased CO_2 injected. CO_2 losses is estimated as the difference between total CO_2 injected and CO_2 produced. Losses may be due to leakages, infrequent power outages, among others [10].

CO_2 can be injected into conventional geological formations and stored deep underground. Most of these conventional geologic formations are at depths greater than 800 m, which eventually converts the injected CO_2 into its supercritical state. The supercritical CO_2 with a higher density than its gaseous state results in a given volume of rock capable of holding more mass of CO_2 [4, 7]. For an effective conventional geological storage, approximately 90–95% of the injected CO_2 for will be sequestered within the reservoir [4, 9, 16].

4.1. Storage mechanisms in conventional reservoirs

Trapping mechanisms encountered in CO_2-storage in conventional geologic formations include [9–11]:

• Physical trapping: hydrodynamic, stratigraphic, or structural) trapping

This involves the migration of generated hydrocarbons from organic matter (source) over long geological periods from the source rock to porous and permeable reservoir rock initially saturated with brine. The accumulated hydrocarbons are trapped below a non-permeable cap rock to prevent further migrations, and the density difference between the fluids separates the fluids into layers with gas on top, followed by oil and brine at the bottom. A similar mechanism is encountered in the case of CO_2 storage, where the less dense supercritical CO_2 plume rises due to buoyancy forces and is prevented from escaping by overlying low permeability cap rock [15]. This mechanism is considered to be relatively fast but requires characterization of the cap rock [2, 3].

• Solubility trapping

CO_2 is widely accepted to be soluble in water, as such, dissolved CO_2 can be safely stored in a geologic formation under solubility trapping. Since the CO_2- saturated brine is denser than the

unsaturated surrounding brine, density difference causes the denser brine to migrate deeper into the formation and slowly dilutes the unsaturated brine through contact. Reservoir pore pressure, temperature, and salinity of formation water are vital for solubility trapping [16]. This process occurs faster than pure diffusion, prevent CO_2 from hydrodynamically separating from other phases, and it is estimated to begin between a year and hundreds of years after CO_2 injection, also dependent on the permeability of the formation in question [2, 20].

• Mineral trapping

This process occurs over longer geological timescales than the other trapping methods, but is equally important [3]. It involves the formation of carbonic acids (H_2CO_3) as a result of CO_2 dissolution in formation brine. The resulting acid is unstable and dissociates to form groups, which react with the formation rock over long periods of time [2, 3]. In situations where, carbonate minerals are precipitated through the reaction, CO_2 is permanently trapped as a result [23].

• Capillary (residual) trapping

In a conventional sandstone oil reservoirs, brine is mostly designated as the wetting phase, while oil and gas are the non-wetting phases. In the case of carbonate rocks, oil is the wetting phase and water and gas are the non-wetting phases. In capillary trapping, the formation wetting phase surrounds the CO_2 and traps it as immobile pore scale bubbles. This process occurs over shorter time scale (right after injection) [15] compared to the other trapping mechanisms [2, 19]. In effect, the rock surface is presumed to be less water-wet in the presence of CO_2 and in the absence of oil [9].

These trapping mechanisms occur in geologic storage including [13, 14]:

• Depleted oil and gas reservoirs

Not only do these geologic formations provide a means for storing CO_2, but also offer economic opportunities as the injected CO_2 recovers additional oil from depleted oil and gas reservoirs. Moreover, additional revenue can be obtained from the cost of selling captured CO_2 to EOR operators to fund the cost of capture technology at industrial facilities and power plants [4, 14, 17]. CO_2 is injected underground and remains immobile due to some of the enumerated trapping mechanisms listed above [3, 20].

• Deep saline formations

Saline aquifers are preferred due to their large capacities and being geographically widespread. These include porous rock formations saturated with brine at greater depths with overlying shale cap rocks, which are impermeable and act as a seal to prevent CO_2 from leaking [4, 17]. The confined CO_2 also undergoes dissolution in the brine, as well as capillary trapping to render the injected CO_2 immobile. A study [2] was carried out to measure the maximum saturation and the form of capillary curve in a CO_2 – Berea sandstone system through coreflood experiments, representative of a storage location. A capillary trapping capacity of 7.8% of the rock volume for CO_2 – Berea sandstone was recorded [2]. This is to say,

if this much is recorded in an unconsolidated formation, how much more there is to expect in a consolidated formation.

- Coal beds

Coal beds are either too deep or too thin to be economically developed, as such, they could offer CO_2 storage potential due to the adsorptive nature of the pore surfaces [4, 13]. In CO_2–enhanced coalbed methane (ECBM) production, CO_2 is injected into deep coal seams to desorb methane gas to be extracted and preferentially adsorb onto the mineral surface for permanent CO_2–storage. Yet they are not thoroughly characterized and are on a small magnitude for CO_2–storage [8, 19, 21].

4.2. Storage criterion

Nonetheless, not all geologic formations will effectively store CO_2 with minimum risks of leaking due to the buoyancy of CO_2 gas. The criteria for secure storage involve some of the following parameters (**Table 1**) as reported in a successful project carried out in Canada [10].

Table 2 summarizes CO_2-EOR and CO_2 storage projects carried out in some major oil basins around the world. A total of 1297 billion barrels of CO_2 has been utilized worldwide for CO_2-EOR, while a total of 370 billion metric tons has been stored/sequestered in the process [4].

4.3. Carbon storage regulation

CO_2 storage site selection and injection are regulated by the U.S. Federal and State agencies, in addition to checking systems for CO_2 capture and storage to reduce the potential risk of stored CO_2 to humans and the environment [1, 10, 18]. Specific regulations and particular tools are commonly implemented to selected reservoirs by different companies and agencies [1, 10].

Furthermore, the Safe Drinking Water Act (SDWA) and the U.S. Environmental Protection Agency (EPA) impose safety requirements on CO_2 injection and monitoring. Whereas, the Underground Injection Control Program (UICP) considers the previous seismic history as a requirement in selecting geologic CO_2 sequestration sites to reduce the risk of small earthquakes as well as the effect of earthquakes on leakage of CO_2. **Table 3** presents a list of monitoring tools used for CO_2-EOR and CO_2 storage projects.

Adequate depth (> 1000 meters)
Strong confining seals
Minimally faulted, fractured or folded
Adequate volume and permeability for storage
No significant diagenesis

Table 1. Criteria for storage on a basin scale [10].

Region	CO_2-EOR (Billion Barrels)	CO_2 Storage capacity (Billion Metric Tons)
Asia Pacific	47	13
Central & South America	93	27
Europe	41	12
FSU	232	66
Middle East/North Africa	595	170
North America/Other	38	11
North America/U.S.	177	51
South Africa/Antarctica	74	21
TOTAL	**1297**	**370**

Table 2. CO_2-EOR and CO_2 storage in major oil basins of the world [4].

Cement integrity logs
Injection logs
Pattern and material balance techniques
Tracer injection/logging
Step rate testing
Fluid levels and reservoir pressure

Table 3. Reservoir monitoring tools used in CO_2-EOR [10].

5. CO_2 storage in unconventional shale reservoirs

As previously mentioned, conventional oil and/gas reservoirs form from the migration of petroleum and natural gas from the source (organic matter) into permeable reservoir rocks. On the other hand, unconventional shale gas/oil serve as both the source and reservoir for natural gas and liquid hydrocarbon (oil and gas condensate). These shale formations are being developed widely for oil and gas production especially in the United States (U.S) and other parts of the world. Moreover, shale formations are much more abundant and widely distributed [17] than deep un-mineable coal seams and/ or depleted oil and gas reservoirs but have not been extensively analyzed for CO_2 sequestration [19]. This is attributed to the ultra-tight nature of shales but the recent advances in horizontal drilling and hydraulic fracturing offers a new perspective into these formations [5, 19].

Shales consist of a mineral matrix (clay, pyrite, carbonate, quartz) embedded with dispersed dark kerogen (organic matter) areas as shown in **Figure 3**. Kerogen is the insoluble solid-phase nanoporous component of organic matter (decomposed plant and animal debris) in

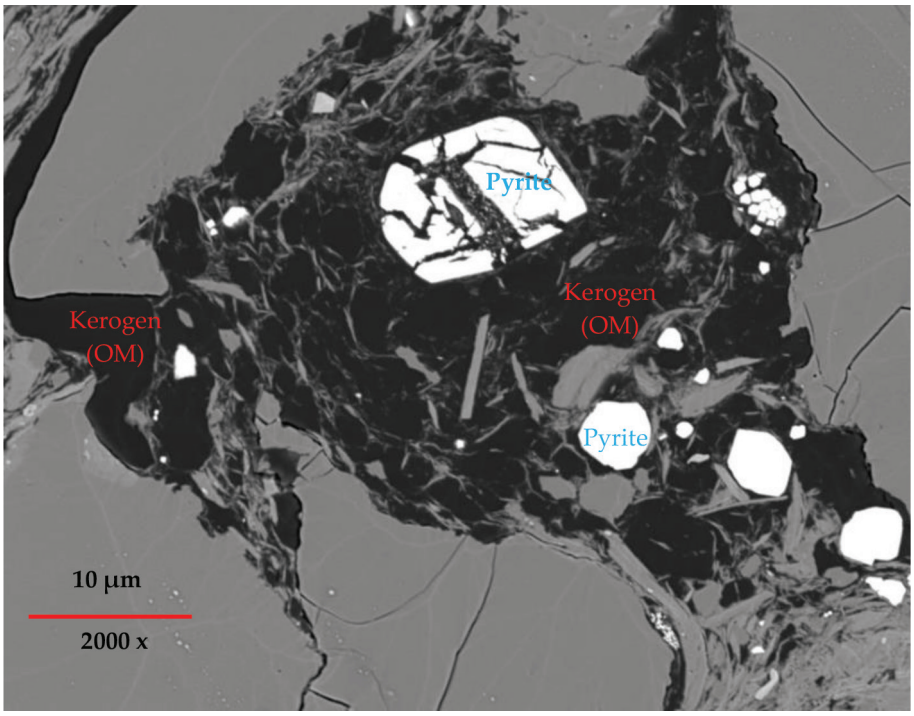

Figure 3. Backscattered electron (BSE) image of Chattanooga shale, Barber County, KS.

shale formations, which controls the gas adsorption capacity. It undergoes different stages of maturity (decomposition) at higher temperatures to produce petroleum and natural gas within the micropores (<2 nm) and mesopores (2–50 nm) [6]. The kerogen pores create a sieve for smaller CO_2 molecules, making shales more attractive for CO_2 sequestration unlike methane (CH_4) and other gas molecules [18, 30]. Thus, shales can adsorb substantial amounts of CO_2 on kerogen as well as fracture surfaces [19, 24]. The level maturity of kerogen is measured by the vitrinite reflectance (% Ro), which indicates the onset of oil (0.6–1.0 Ro%), wet gas (<0.80% Ro) and natural gas (>1.4% Ro) generations, respectively [20, 21]. Gas from shale formations are either thermogenic (generated from cracking of organic matter or the secondary cracking of oil) or biogenic (generated from microbes) [22, 26].

Because the source rock doubles as the reservoir, shales are characterized as very low permeability formations, which form strong confining seals in their own right but have surface adsorptive characteristics. As such, they require the creation of hydraulic fractures to form conduits for introducing fluids and producing them to the surface through horizontal wells. Hydraulic fracturing cracks the shale rock through injections of water, sand and chemicals at high pressure [16]. Horizontal wells with multi-stage hydraulic fractures can then be used to inject CO_2 for storage in depleted shale gas and oil reservoirs. The horizontal wells as opposed to vertical wells in conventional geologic formations add to the effectiveness of CO_2

sequestration in shales since the horizontal wells contact more of the shale formation and as a result, increase the subsurface production area of the well [19]. More so, CO_2 sequestration in shales would not require new infrastructure unlike in conventional saline aquifers [19, 20].

Most of the shale formations are located at greater depths, where the injected CO_2 is in its supercritical state, which is much preferred for both CO_2 – enhanced gas/oil recovery (EGR)/ EOR in addition to CO_2 sequestration. The injected CO_2 for EGR/EOR in organic-rich shales adsorb onto the rock surface, while concurrently releasing methane gas (CH_4) and/ or oil for natural gas and oil productions, respectively [8, 22]. Furthermore, since most of the injected CO_2 would be adsorbed to the surface of kerogen rather than exist as free gas, the problem of leakage is minimized [8]. Hence, CO_2 sequestration in shales is feasible but requires knowledge of the characteristics of different shale formations as well as gas-water-rock interactions, multiphase flow, and reservoir modeling, monitoring and verification [22, 25].

Tao and Claren [19] introduced a computational method based on historical and projected methane (CH_4) production to estimate the capacity of CO_2 sequestration in Marcellus shale in eastern United States. From the results obtained, the Marcellus shale is expected to store between 10.4 and 18.4 Gt of CO_2 (approximately 50% of total US CO_2 emissions) between now and 2030. Another point to note from Tao and Claren [19] was that injected CO_2 moves through the shale formation faster than producing CH_4 through mass transfer kinetics, which enhances CO_2 sequestration process in shales. In addition, other major shale plays like Barnett, Eagle Ford, Woodford, could provide incremental storage capacity.

Nuttal [22] performed experiments to estimate CO_2 sequestration capacity in organic-rich Devonian black shales of Eastern Kentucky to be 6.8 Gt [19]. CO_2 was found to adsorb onto clay and kerogen surfaces. A direct correlation was observed between CO_2 adsorptive capacity and the total organic carbon (TOC), where CO_2 adsorption capacity increases with increasing TOC.

Kang et *al.* [6] examined shale capacity in organic-rich shales and their added advantage of allowing linear CO_2 molecules to penetrate smaller pores otherwise inaccessible to other hydrocarbon gases. Moreover, molecular interaction of CO_2 and kerogen ensures enhanced adsorption for CO_2 sequestration in shales. Injected gas (CO_2) molecules move through the shale formation through either the organics or inorganics (or both in most cases). In the organics, CO_2 dissolves into kerogen and diffuses into the kerogen nanopores, whereas, in the inorganics, CO_2 flows through irregularly shaped pores of clays, pyrite fambroids, quartz, and carbonates. Gas permeation and history-matching pressure pulse decay experiments revealed that significant amounts of CO_2 gas reached the organics through the inorganic pores.

Busch et *al.* [5] conducted diffusive transport and gas sorption experiments on shale samples. Effective diffusion coefficients increased (implies irreversible storage of CO_2) with a corresponding decrease in the concentration of bulk CO_2 volume in the sample. The decrease in bulk CO_2 volume is attributed to the dissolution of CO_2 in formation water (brine), adsorbed to clay and kerogen surfaces or undergoes geochemical reactions.

Furthermore, reservoir models can be built and used to predict viable CO_2 storage in shale reservoirs to model diffusivity, gas-water-rock interactions, and adsorption/desorption characteristics, among others. Notably, the presence of clay bound water is known to change the

gas sorption properties in coal formations so it is likely to manifest in shales as well. These phenomena could also be well understood through experimental methods [16, 19].

With these new insights, CO_2 sequestration in shale formations looks promising, however, the underlying physics of CO_2 sequestration in kerogen nanopores, where most of the sequestration takes place is much needed. A better understanding of the fluid dynamics in kerogen nanopores and predicting effective transport properties (diffusivity, permeability, etc.) is of utmost importance to practical CO_2 sequestration applications in shales. Also, it would aid in capitalizing on the full potential of CO_2 –EGR/EOR in organic-rich shales. Therefore, the application of lattice Boltzmann method (LBM) for CO_2 sequestration in kerogen nanopores focusing on the effect of adsorption was applied.

5.1. Mechanisms of CO_2 sequestration in shales

In addition to the trapping mechanisms in conventional reservoirs, organic-rich shales have an added advantage of trapping CO_2 through adsorption in the presence of kerogen [30]. Kerogen is the insoluble component of organic matter, and measured in the lab as the total organic carbon (TOC) through pyrolysis. Thus, both hydrodynamic trapping and trapping through adsorption are dependent on the wettability of CO_2 in in shales.

Tao and Claren [19] developed a linear relationship between TOC and adsorption capacity using a number of published data sets as input into (Eqs. (2) and (3)), respectively for methane (CH_4) and carbon dioxide (CO_2).

$$[CH_4](cm^3/g) = 3.04 + 0.35(TOC(\%)) \tag{2}$$

$$[CO_2](cm^3/g) = 0.08 + 1.72(TOC(\%)) \tag{3}$$

The resulting plot showed the regression line of CO_2 adsorption capacity to be steeper than that of CH_4, implying that CO_2 is able to diffuse more readily than CH_4 into the porous kerogen due to its smaller molecular diameter [19]. Accordingly, we produced a TOC vs. gas adsorption capacity plot but with a focus on the level of TOC and its effect on gas adsorption capacity. Shale formations are in abundance and have diverse geologic settings throughout the U.S. (Appalachian basin, Williston basin, Illinois basin, Michigan basin, Permian basin, and Gulf Coast Region) for EOR and associated CO_2 storage [19, 23] but vary in kerogen content (TOC) and this variation in TOC has been found to impact the storage capacity of shales.

Figure 4 shows the TOC – gas adsorption capacity for a number of published TOC data [5, 19, 22, 23] ranging from low TOC (<1 wt. %), medium TOC (1 wt. % < TOC < 10 wt. %), high TOC (10 wt. % < TOC < 20 wt. %), and ultrahigh TOC (>20 wt. %) [24]. Highest CO_2 adsorption capacity is seen in the ultrahigh TOC region, followed by significant adsorption capacity in the high TOC region; the least adsorption capacity is observed at low TOC region. This implies that, the higher the kerogen content in shales, a significant amount of CO_2 sequestration is expected through adsorption trapping with subsequent production of significant amounts CH_4 displaced in the process. Therefore, conventional structural trapping becomes dominant

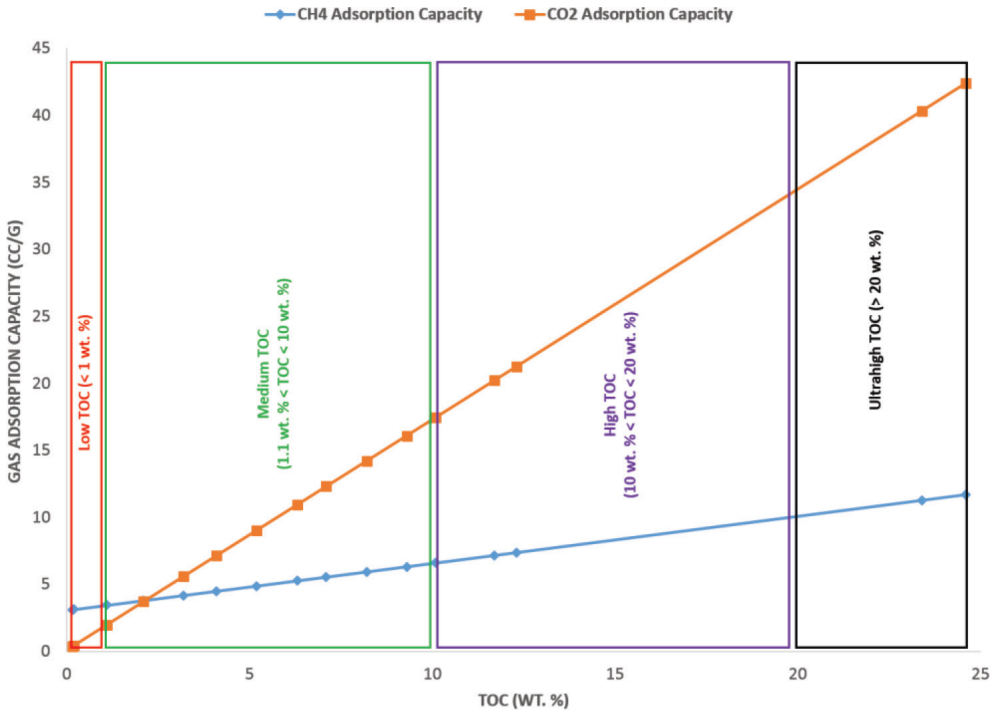

Figure 4. Gas adsorption capacity as a function of different levels of TOC.

in low TOC regions, where shale only serves as a cap rock/seal to prevent dissolved CO_2 from leaking to the surface since the mechanism of adsorption into porous kerogen (TOC) surface is close to negligible. On the other hand, within high TOC (>2 wt. %) regions, the adsorption trapping mechanism onto the kerogen surface prevails and render shale as storage medium in itself. In other words, shales with high TOC tend to be strongly CO_2-wet, whereas shales with low TOC content exhibit water-wet conditions, with medium TOC in between strongly CO_2 –wet and water-wet conditions [24]. Furthermore, the presence of interlayering clay minerals (illite) in shales also creates a large surface area for adsorption, although the weight of TOC has a much larger influence [25].

The properties of supercritical CO_2 inside small pores are of interest for subsurface carbon storage and as such require an understanding of the processes that govern the gas transport process [19, 23]. Molecular dynamics (MD) among other microscopic computational fluid dynamics as well as analytical models based on Fick's law for gas have been applied to understand the diffusion of CO_2 and CH_4 into organic pores. While, molecular dynamics simulates kerogen pore structures with the use of molecular sieves to investigate gas transport, analytical models modify continuum approaches by incorporating slip flow and diffusion. However, molecular dynamics is not feasible to simulate gas flow in porous media at large scale due to computational time and memory constraints [25, 26] and analytical models

fall short of capturing molecular pore wall effects. On the other hand, the lattice Boltzmann method (LBM), a mesoscopic numerical method is more flexible and less time consuming since a unit of gas molecules is assigned a distribution function for simulation [25, 26].

As previously outlined, the injected gas first contacts the fracture/matrix interface and then chooses to either (1) dissolve into the organic material (kerogen) and diffuse through a nanopores network or (2) enter the inorganic material and flow through a network of irregularly shaped voids [6, 18]. Therefore, the interaction of supercritical CO_2 ($scCO_2$) with porous kerogen needs to be investigated for long-term reservoir storage of CO_2 in organic-rich shales. We provide a simulation study that reveals the interaction of $scCO_2$ with porous kerogen focusing on two key features of adsorption and diffusion.

5.2. Lattice Boltzmann simulation (LBS) of CO_2 sequestration

The lattice Boltzmann method (LBM) is a numerical method for simulating fluid at the molecular scale. This method is ideal for simulating gas flow in nanoporous kerogen since the continuum flow (Darcy's law) fails due to dominating pore-wall effects at the microscale. LBM stems from the Boltzmann kinetic theory of gases, where fluids are assumed to be made up of a large number of small particles in random motion, which undergo elastic collisions to conserve mass and momentum [19, 23, 24]. However, the LBM replaces the fluid molecules with fractious particles to reduce the number of possible particles to a handful [28]. The fractious particles are then confined to the nodes of the lattice and assigned lattice velocities (e_i) at each node as shown in **Figure 4**, where the direction index $i = 0, 1, \ldots, 8$, for a D2Q9 model [29] (**Figure 5**). Following the kinetic theory, the fractious particles stream along defined lattice links and collide locally at varying lattice sites [23–25]. The streaming and collision of fluid particles by the Bhatnagar-Gross-Krook (BGK) approximation gives the lattice Boltzmann BGK equation as [19, 23–26].

$$f_i(x + e_i\,\Delta t, t + \Delta t) - f_i(x, t) = -\frac{1}{\tau}\left[f_i(x, t) - f_i^{eq}(x, t)\right] \tag{4}$$

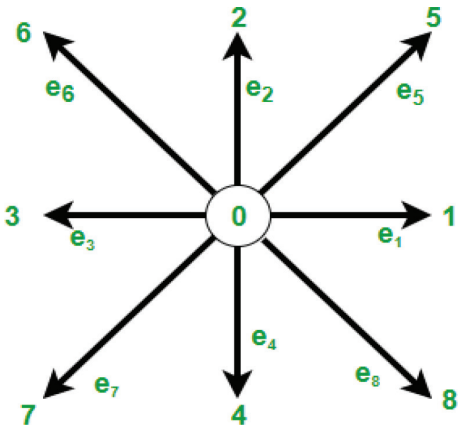

Figure 5. D2Q9 (2-D, 9-velocities) lattice nodes and velocities. Modified from [29].

where, $f_i(x, t)$ is the density distribution function, $f_i^{eq}(x, t)$ is the equilibrium distribution function, τ is the relaxation time. The left-hand side (LHS) of (Eq. (2)) represents the streaming step, while the right-hand side (RHS) constitutes the collision step.

In effect, collision of fluid particles is considered as a relaxation towards a local equilibrium, and defined for every model with varying dimensions (2-D, 3-D) and velocities (5, 9, 15, etc.).

The LBM models the distribution of and changes in the density function, from which the velocity profile is determined. Accordingly, the macroscopic fluid density and velocity are given respectively as [19, 23, 24].

$$\rho = \sum_{i=0}^{8} f_i \tag{5}$$

$$u = \frac{1}{\rho} \sum_{i=0}^{8} f_i e_i \tag{6}$$

where, ρ is the macroscopic fluid density and u is the macroscopic fluid velocity.

Several works [18, 29] have been carried out on modeling the convection problem encountered in deep saline aquifers during CO_2 sequestration with the lattice Boltzmann method (LBM). The findings include the fact that brine with a high CO_2 concentration was found to invade into the underlying unsaturated brine, causing an increase in the interfacial area between the CO_2–rich brine and CO_2 – deficient brine. In effect, this phenomenon enhanced the migration of CO_2 into the fracture and pores.

However, in organic-rich shales, most of the sequestration process takes place within the kerogen nanopores through adsorption [30, 31]. In so doing, there is the need to understand the interaction of supercritical CO_2 ($scCO_2$) with porous kerogen for long-term reservoir storage of CO_2 in organic-rich shales.

In a typical kerogen nanopore, the velocity is discontinuous at the pore wall due to the mean free path of the gas molecules exceeding the characteristic length (pore size). This phenomenon is characterized by the Knudsen number (K_n); slip flow regime falls within $0.001 < K_n < 0.1$. For chosen characteristic length 20 nm for our LBS ($K_n = 0.0243$), fluid flow falls within the slip flow regime. Slip flow boundary condition was modified for CO_2 molecules, which are predicted to not reflect at the walls but rather adsorb and desorb after some time lag [26, 27]. In effect, the velocity of the pore wall is defined to be dependent on the surface diffusion coefficient of CO_2 gas as well as Langmuir adsorption parameters based on the amount of adsorbed gas. Hence, the slip velocity at the pore-wall is given by [26, 27, 30].

$$u_{slip} = (1 - \alpha)\, u_g + \alpha u_w \tag{7}$$

where, u_{slip} is the slip velocity, u_g is the fluid velocity away from the wall, u_w is the local wall velocity dependent on the surface diffusion coefficient, and $\alpha$is the amount of adsorbed gas at the solid surface through Langmuir isotherm.

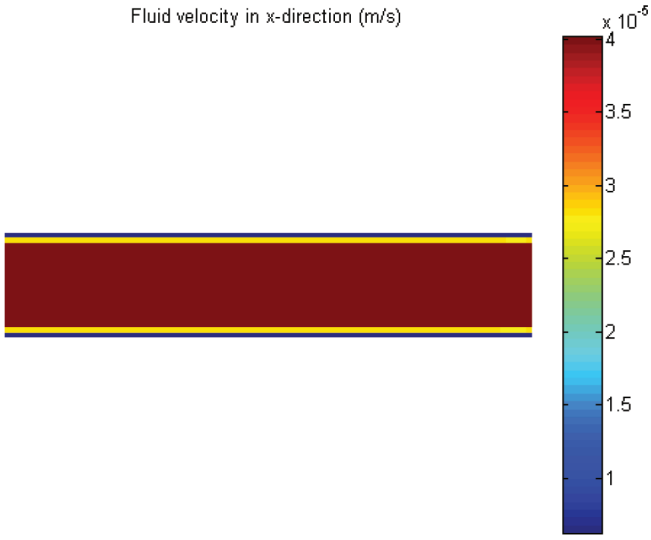

Figure 6. Composite velocity distribution of both CH_4 (center) and CO_2 (at the walls) in a 20 nm pore-slit.

Marcellus shale reservoir conditions were implemented at a high pressure of 12 MPa and temperature of 300 K. The D2Q9 LBM diffusion coefficient is known to be given in (Eq.(8)) and is directly comparable to the kinematic viscosity [28, 32].

$$D = \frac{1}{3}\left(\tau_\sigma - \frac{1}{2}\right) \tag{8}$$

where, D is the diffusion coefficient of the D2Q9 LBM and τ_σ is the relaxation time for each fluid component.

A 20-nm pore-slit is filled with both CH_4 and CO_2 at 12 MPa. Hydrodynamic velocity boundary condition is implemented at the upper and lower walls, while the pressure boundary condition is applied to the east and west ends. **Figure 6** shows the static velocity profile of both fluids in the pore-slit; CO_2 occupies the surface of the pore walls on both ends as the wetting phase, while methane occupies the center as the non-wetting phase.

Estimating the amount of adsorbed gas for CO_2 and CH_4, respectively, it was found that CO_2 adsorption capacity was much more than that of CH_4 for the same pore dimension and prevailing temperature and pressure. Furthermore, the diffusion coefficient CO_2 at $\tau = 1$ is higher than the diffusion coefficient of CH_4 at $\tau = 0.8$. The estimated magnitude of CH_4 diffusion coefficient is given in the range of 10^{-13}–10^{-10} m^2/s in carbon molecule sieves [19].

6. Conclusions

CO_2 sequestration in organic-rich shales to mitigate greenhouse gas (GHG) effects is proven to be very feasible through experimental and numerical simulations. Our literature review

and LBS suggest that organic-rich shales are capable of storing CO_2 in substantial quantities in its adsorbed state in the presence of higher TOC levels. In addition to shales being widely distributed and in abundance, the natural confining seals of the formation reduces the risk of leakage. On the other hand, CO_2-EGR/EOR can be achieved as part of the CO_2 sequestration process; CO_2-EGR/EOR produces relatively clean fuel and sustains energy demands.

However, to accurately benefit from CO_2 – sequestration in organic-rich shales, there is the need to overcome developmental challenges and understand the rock-fluid and fluid–fluid interactions in organic-rich shales for large scale pilot test and implementation.

Acknowledgements

We acknowledge the support of the Tertiary Oil Recovery Program (TORP) and Kansas Interdisciplinary Carbonates Consortium (KICC) at the University of Kansas. We would also like to thank Erin Honse (Fischer Scientific, formerly FEI) for acquisition of BSE images of our shale sample.

Conflict of interest

The authors declare no conflict of interest.

Notes

The authors declare no competing financial interest.

Appendices and nomenclature

EGR/EOR	enhanced gas recovery/enhanced oil recovery
OOIP	original oil-in-place
ECBM	enhanced coalbed methane
CO_2	carbon dioxide
$scCO_2$	supercritical CO_2
CH_4	methane
Gt	giga tons
TOC	total organic carbon/content

Ro %	vitrinite reflectance
LBM	lattice Boltzmann method
LBS	Lattice Boltzmann simulation
BGK	Bhatnagar-Gross-Krook
$f_i(x, t)$	velocity distribution function
$f_i^{eq}(x, t)$	equilibrium distribution function
τ	relaxation time
e_i	lattice velocities
ρ	macroscopic density
u	macroscopic velocity
GHG	greenhouse gas
MPa	mega Pascal
K	Kelvin
Kn	Knudsen number
nm	nanometer
u_{slip}	slip velocity
D	diffusion coefficient of D2Q9 LBM
D2Q9	2-dimensional, 9 velocity/speed model

Author details

Cudjoe Sherifa* and Barati Reza

*Address all correspondence to: reza.barati@ku.edu

University of Kansas, Lawrence, USA

References

[1] U.S. Department of Energy. Carbon Capture, Utilization, and Storage: Climate Change, Economic Competitiveness, and Energy Security; 2016

[2] Pentland CH. Measurements of Non-wetting Phase Trapping in Porous Media. London, United Kingdom: Imperial College London; 2010

[3] Bachu S. Aquifer disposal of CO_2: Hydrodynamic and mineral trapping. Energy Conversion and Management. 1994;**35**(4):269-279

[4] Kuuskraa VA, Godec ML, Dipietro P. 2 utilization from 'next generation' CO_2 enhanced oil recovery technology. Energy Procedia. 2013;**37**:6854-6866

[5] Busch A et al. Carbon dioxide storage potential of shales. International Journal of Greenhouse Gas Control. 2008;**2**(3):297-308

[6] Kang SM, Fathi E, Ambrose RJ, Akkutlu IY, Sigal RF. Carbon dioxide storage capacity of organic-rich shales. SPE Journal. December 2011:842-855

[7] Carbon Capture. Center for Climate and Energy Solutions (C2ES). [Online]. Available from: https://www.c2es.org/content/carbon-capture/. [Accessed: March 13, 2018]

[8] DiPietro P, Balash P, Wallace M. A note on sources of CO_2 supply for enhanced-oil-recovery operations. SPE Economics & Management. March 2012;**2012**:69-74

[9] (EIA) Hodge T. Natural gas expected to surpass coal in mix of fuel used for U.S. power generation in 2016. Today in Energy. [Online]. 2016. Available: https://www.eia.gov/todayinenergy/detail.php?id=25392. [Accessed: March 13, 2018]

[10] Melzer LS. Carbon dioxide enhanced oil recovery (CO_2 EOR): Factors involved in adding carbon capture, utilization and storage (CCUS) to enhanced oil recovery. Science and Engineering Ethics. February 2012:1-23

[11] U. S. D. of Energy. Carbon dioxide enhanced oil recovery. Netl. 2017:1-36

[12] Sohrabi M, Kechut NI, Riazi M, Jamiolahmady M, Ireland S, Robertson G. Safe storage of Co_2 together with improved oil recovery by Co_2-enriched water injection. Chemical Engineering Research and Design. 2011;**89**(9):1865-1872

[13] Elsharkawy AM, Poettmann FH, Christiansen RL. Measuring minimum miscibility pressure: Slim-tube or rising-bubble method? SPE/DOE Enhanced Oil Recovery Symposium. 1992;**5**:443-449

[14] Hawthorne SB, Gorecki CD, Sorensen JA, Miller DJ, Harju JA, Melzer LS. Hydrocarbon mobilization mechanisms using CO_2 in an unconventional oil play. Energy Procedia. 2014;**63**:7717-7723

[15] Chen C, Zhang D. Pore - scale simulation of density - driven convection in fractured porous media during geological CO_2 sequestration. Water Resources Research. April 2010;**46**:1-9

[16] Eshkalak MO, Aybar U, Eshkalak MO. Carbon dioxide storage and sequestration in unconventional shale reservoirs. Journal of Geosciences and Environment Protection. 2015;**3**(1):7-15

[17] Khosrokhavar R, Griffiths S, Wolf KH. Shale gas formations and their potential for carbon storage: Opportunities and outlook. Environmental Processes. 2014;**1**(4):595-611

[18] Pu H, Wang Y, Li Y. How CO_2 storage mechanisms are different in organic shale: Characterization and simulation studies. Society of Petroleum Engineers EAGE … SPE EUROPEC 2018 at the 80th EAGE Conference & Exhibition. 2016

[19] Tao Z, Clarens A. Estimating the carbon sequestration capacity of shale formations using methane production rates. Environmental Science & Technology. 2013;**47**(19):11318-11325

[20] Jarvie DM. Shale resource Systems for oil and gas: Part 1—shale-gas resource systems. Shale Reservoirs: Giant Resources for the 21st Century. AAPG Memoir. 2012:69-87

[21] Jarvie DM, Hill RJ, Ruble TE, Pollastro RM. Unconventional shale-gas systems: The Mississippian Barnett shale of north-Central Texas as one model for thermogenic shale-gas assessment. American Association of Petroleum Geologists Bulletin. 2007;**91**(4):475-499

[22] Nuttall BC. Analysis of Devonian black shales in Kentucky for potential carbon dioxide sequestration and enhanced natural gas production. Lexington, Kentucky; 2005

[23] Lopez AJ. Financial assistance funding opportunity announcement (FOA); 2018

[24] Arif M, Lebedev M, Barifcani A, Iglauer S. Influence of shale-total organic content on CO_2 geo-storage potential. Geophysical Research Letters. 2017;**44**(17):8769-8775

[25] Aljamaan H, Holmes R, Vishal V, Haghpanah R, Wilcox J, Kovscek AR. CO_2 storage and flow capacity measurements on idealized shales from dynamic breakthrough experiments. Energy and Fuels. 2017;**31**(2):1193-1207

[26] Javadpour F, Fisher D, Unsworth M. Nanoscale gas flow in shale gas sediments. Journal of Canadian Petroleum Technology. 2007;**46**(10):55-61

[27] Guo Z, Shu C. Lattice Boltzmann Method and its Applications in Engineering. Vol. 3. Singapore: World Scientif Publishing Co. Pte. Ltd; 2013

[28] Sukop MC, Thorne DT. Lattice Boltzmann Modeling. 2006;**79**(1 Pt 2)

[29] Mohamad AA. Lattice Boltzmann Method Fundamentals and Engineering Applications with Computer Codes. New York: Springer; 2011

[30] Fathi E, Akkutlu IY. Lattice Boltzmann method for simulation of shale gas transport in Kerogen. In: Proceedings of the SPE Annual Technical Conference and Exhibition. 2013;**4**(1):27-37

[31] Cudjoe S, Barati R. Lattice Boltzmann simulation of CO_2 transport in kerogen nonporous - An evaluation of CO_2 sequestration in organic-rich shales. Journal of Earth Science. 2017;**28**(5):926-932

[32] S M, Haibo Huang X-YL. Single-component multiphase Shan-Chen-type model. Multi phase Lattice Boltzmann Methods: Theory and Application. First, no. 2012. Chichester, West Sussex, UK: John Wiley & Sons, Ltd; 2015. pp. 18-64